Hindawi Publishing Corporation
Journal of Nanomaterials
Volume 2012, Article ID 536810, 6 pages
doi:10.1155/2012/536810

Research Article

Electrodeposition and Low-Temperature Post-Treatment of Nanocrystalline SnO_2 Films for Flexible Dye-Sensitized Solar Cells

Shengjun Li, Yongjun Li, Zeng Chen, Junhui Liu, and Weifeng Zhang

Key Laboratory of Photovoltaic Materials of Henan Province and School of Physics and Electronics, Henan University, Kaifeng 475001, China

Correspondence should be addressed to Weifeng Zhang, wfzhang@126.com

Received 1 November 2011; Accepted 28 December 2011

Academic Editor: Anukorn Phuruangrat

SnO_2 porous films were electrodeposited on Ti substrate using pulse-potential technique. These deposited films were dealt with different post-treatments. The effects of the post treatments were investigated through X-ray diffraction, FE-SEM, and Raman spectra. These investigations showed that crystal nanoporous SnO_2 films were obtained through low-temperature post-treatment process. The photoelectric conversion efficiency of the SnO_2 film treated with both the water vapour treatment and ultraviolet illumination was improved to be 0.35% which was comparable with the conversion efficiency of the film sintered at 550°C.

1. Introduction

Dye-sensitized solar cells (DSCs) have attracted great scientific and technological interests as photovoltaic devices for their utilization of nontoxic materials, simple preparation process, and high photoelectric conversion efficiency up to 11% [1, 2]. Conventionally, the working electrode was prepared based on the substrate of transparent conductive glass which cannot be bended and tends to be crashed. As a substitute, flexible substrate, such as poly(ethylene terephthalate) coated with indium-doped tin oxide (ITO/PET), has been adopted in the DSCs [3, 4]. The PET substrate is lightweight and flexible, but it cannot withstand the temperature above 150°C. To achieve high-quality nanoporous photoelectrode at low temperature, various methods have been developed, such as hydrothermal synthesis, chemical vapor deposition, physical vapor deposition, and electrodeposition [5–7]. In contrast with other techniques, the electrodeposition method shows many advantages, for example, it is usually carried out below 100°C and can give rigid control on film thickness and composition. The electrodeposited semiconductor oxides show high porosity and fine substrate adhesion. Various metal oxides, such as TiO_2, ZnO, In_2O_3, and ZrO_2, have been successfully electrodeposited [7–10]. During the electrodeposition process, the electrons keep flowing through the nanoporous film. So the electrodeposited film is expected to possess fine electron transport properties even without high-temperature sintering [8, 11].

SnO_2 has been extensively used in gas sensors and lithium ion batteries for its transparent property and high electronic mobility [12–15]. The application of SnO_2 in DSCs has also been reported [16–19]. Generally, the SnO_2 films show low photoelectric conversion efficiency because of the severe charge recombination and low conduction band edge [20, 21]. But these drawbacks could be overcome by the surface coating of other oxides, such as Al_2O_3, ZnO, and MgO [22, 23]. More importantly, highly crystallized SnO_2 could be obtained at low temperature, so SnO_2 should be a kind of suitable photoanode material for flexible DSCs. In this paper, we electrodeposited SnO_2 film and posttreated the film though various processes. Ti foil was selected to be the substrate of nanocrystalline SnO_2 films for the comparison of various post-treatment processes. After the water vapour treatment with HNO_3 and UV light irradiation, the photoelectric properties were comparable with that of the high-temperature-treated electrodes.

2. Experimental

2.1. Preparation and Characterization of SnO_2 Films. The preparation of nanocrystalline SnO_2 films was carried out with a simple three-electrode system. Ti sheet (thickness of 0.1 mm) and Pt sheet were used as working and counter electrode, respectively. The distance between the working electrode and the counter electrode was controlled to be about 3.5 cm. Ag/AgCl electrode with saturated potassium chloride aqueous solution worked as the reference electrode. The electrolyte consisted of 0.05 M $SnCl_2 \cdot 2H_2O$ and 0.1 M HNO_3. The deposition temperature was fixed at 75°C by an oil bath. The Ti sheet which was used as flexible metal substrate for nanocrystalline SnO_2 film was ultrasonically cleaned in detergent solution, acetone, and deionized water, sequentially. The exposed surface area of the working electrode was about 1.5 cm^2. Electrochemical deposition experiments were carried out with CHI660C electrochemical workstation (Shanghai Chen-Hua Instrument Co, China). Pulse-potential technique was adopted in the deposition process with a high potential of −0.1 V (versus Ag/AgCl) and a low potential of −0.6 V (versus Ag/AgCl). The pulse time was 10 s and deposition time was 2 h.

The as-grown SnO_2 films were yellow. The films were dried in air and treated as the following process: (1) water vapour treatment in an autoclave with 25 mL deionized water for 12 hours at 150°C (pure water vapour treatment), (2) water vapour treatment in an autoclave with 25 mL 0.3 M HNO_3 aqueous solution for 12 h at 150°C (HNO_3 treatment), (3) UV light irradiation treatment at 258 nm for 20 min after the water vapour treatment with HNO_3 solution (UV-treatment), and (4) sintering at 550°C for 1 h in air. After the post treatment, the electrodeposited SnO_2 films turned to be white.

The crystalline phase of the samples was characterized by X-PertPro X-ray diffractometer with a monochromatized Cu Kα irradiation ($\lambda = 0.154145$ nm) and morphologies were determined using HitachiS-4300F field emission scanning electron microscope (FE-SEM). The Raman spectra were measured by a laser Raman spectrometer (Renishaw-1000) at an output power of a 457.5 nm solid-state laser.

2.2. Fabrication and Characterization of Dye-Sensitized Solar Cells. For DSCs fabrication, the samples were immersed in a 5×10^{-4} mol L^{-1} ethanol solution of N3 dye for 24 h. A transparent Pt counter electrode was prepared by spreading 5 m mol L^{-1} H_2PtCl_6 aqueous solution on an FTO glass substrate and pyrolyzed at 390°C for 15 min. The mixture of 0.6 M dimethylpropylimidazolium iodide, 0.1 M iodine, 0.5 M 4-*tert*butylpyridine, and 0.1 M lithium iodide in methoxy acetonitrile was selected to be the electrolyte of DSCs.

The photoelectrochemical characteristics of DSCs were measured by the photocurrent-voltage curve ($I-V$ curves) measurement with CHI660C Electrochemical Workstation under the simulated solar light. A 500 W xenon lamp was used as the light source. The incident light intensity was 100 mW cm^{-2} measured by a Radiation Meter (FZ-A, Beijing Normal University, China) and the active cell area was 0.25 cm^2. The electrochemical impedance spectra (EIS) were also carried out with CHI660C. The impedance measurement of DSC was recorded at the open circuit voltage under light illumination over a frequency range of 0.05–1 M Hz with ac amplitude of 10 mV.

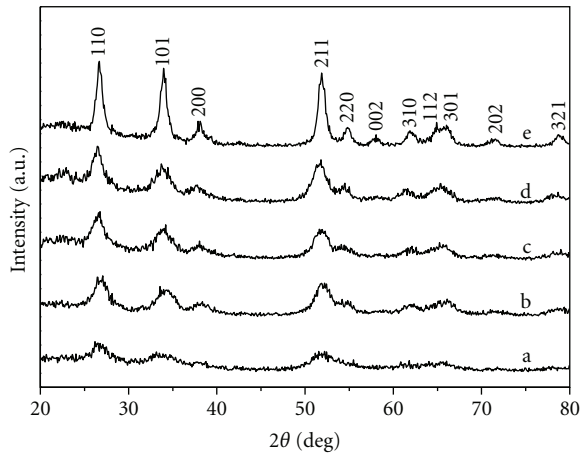

Figure 1: XRD images of the electrodeposited SnO_2 films obtained at different post treatment conditions (a) untreated, (b) pure water vapour treatment, (c) HNO_3 treatment, (d) UV-treatment, and (e) calcined at 550°C.

3. Results and Discussion

The crystallinity of the SnO_2 film before and after post treatment was investigated by X-ray diffraction which is shown in Figure 1. The electrodeposited SnO_2 film without any post treatment already shows the property of crystalline (shown in Figure 1 curve a), but the reflect peaks are weak and broad. So, it is necessary to deal with the deposited films with post treatments. Here, four different post treatment processes were adopted: water vapour treatment with pure water at 150°C (curve b), water vapour treatment with 0.3 M HNO_3 solution at 150°C (curve c), water vapour treatment with 0.3 M HNO_3 solution at 150°C, and UV-treatment (258 nm) for 20 min (curve d), sintering at 550°C for 1 h (curve e). After water vapour treatment, the diffraction peak intensity of SnO_2 became stronger which indicated the enhancement of crystallinity degree. In addition, the diffraction peak intensity of electrodeposited SnO_2 films treated with HNO_3 treatment and UV-treatment was further improved.

Figure 2 shows FE-SEM images of the SnO_2 films obtained through different post-treatment processes. After pure water vapour treatment, crystal nanoporous SnO_2 film was obtained. But the SnO_2 particles exist in an agglomeration state. The particle size is as large as about 70–100 nm which is disadvantageous for the absorption of dye. With the addition of HNO_3 in the water vapour treatment process, more micropores were formed which facilitated the infiltration electrolyte. At the same time, the particle size of SnO_2 was decreased for the adsorption of more dye molecular. Comparing the FE-SEM images of the other three post-treatments, there was no obvious difference.

Table 1: Performance characteristics of DSCs based on the nanocrystalline SnO_2 film under different post treatment processes.

Post treatment conditions	J_{sc} (mA cm^{-2})	V_{oc} (mV)	FF	η (%)
Pure water vapour treatment	0.60	329	0.48	0.09
HNO_3 treatment	1.11	329	0.62	0.23
UV-treatment	1.65	340	0.63	0.35
Calcined at 550°C	4.22	334	0.37	0.52

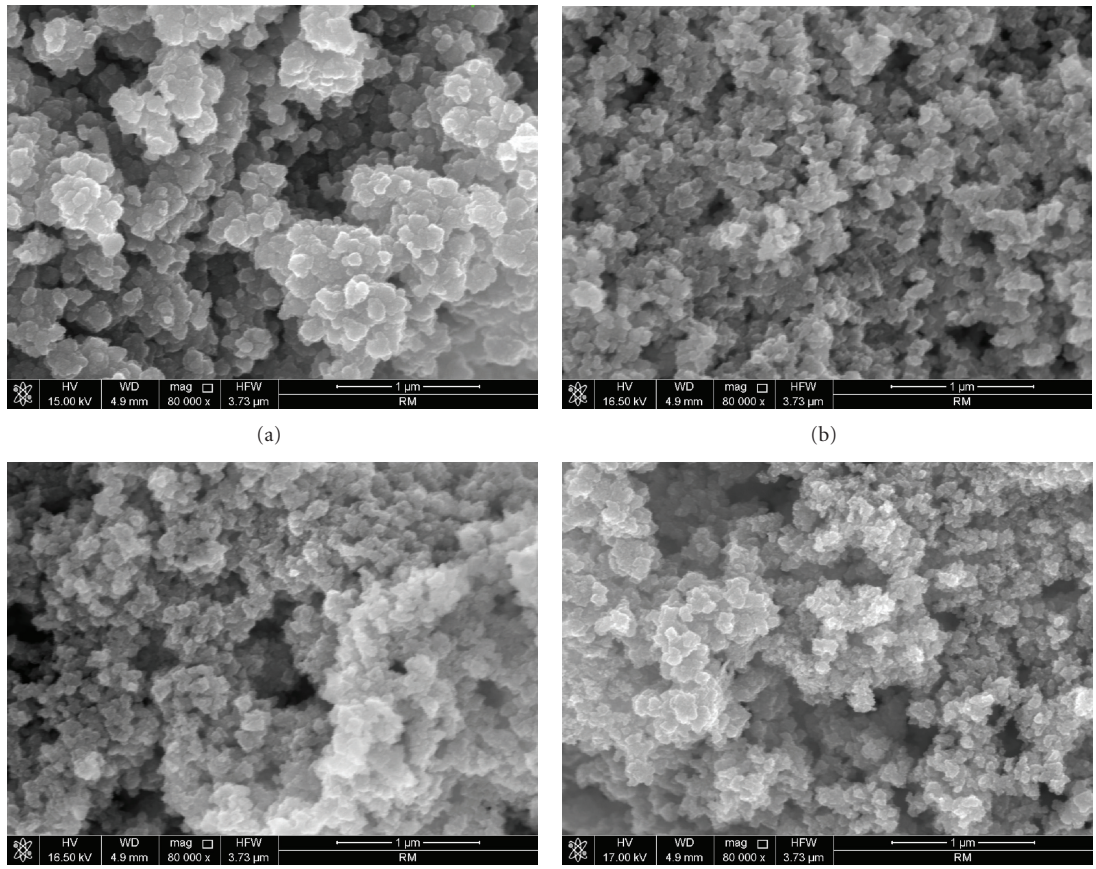

Figure 2: FE-SEM of the electrodeposited SnO_2 films obtained at different conditions, (a) pure water vapour treatment, (b) HNO_3 treatment, (c) UV-treatment, and (d) calcined at 550°C.

In order to give more insight into the structural change of the SnO_2 films obtained through different post treatments, Raman spectra are presented in Figure 3. The scattering peak at about 557 cm^{-1} of the low-temperature-treated films disappears in the spectrum of the film sintered at 550°C which might be caused by the smaller particle size of the films without high-temperature crystallization process [24]. However, the SnO_2 film treated with pure water vapour shows larger particle size in SEM spectra than that of the high-temperature sintered films. This phenomenon further suggested that the SnO_2 existed as an agglomeration state though small SnO_2 particles were electrodeposited from the electrolyte. The peak at 1600 cm^{-1} corresponded to the vibration of the OH units absorbed at the surface of SnO_2 nanoparticles which facilitated the absorption of dye [24]. In addition, an extra peak was observed at the frequency of 1045 cm^{-1} after the HNO_3 water vapour treatment. This new scattering peak should be associated with the interaction of the HNO_3 and SnO_2 nanoparticles. The addition of HNO_3 had made some significant changes for the SnO_2 films.

The SnO_2 films obtained under different post treatment were sensitized with N3 dye and used to assemble DSCs. Figure 4 shows the current-voltage characteristics of the cells under simulated solar illumination (at 100 mW cm^{-2}) and Table 1 gives the characteristic parameters, that is, open circuit voltage (V_{oc}), short circuit current (J_{sc}), fill factor (FF), and overall light to electricity conversion efficiency (η). The SnO_2 films treated with pure water vapour show low J_{sc} (0.60 mA cm^{-2}) and fill factor (0.48). With the addition of HNO_3, the J_{sc} and fill factor were both enhanced to be 1.02 mA cm^{-2} and 0.64. The improvement of the short circuit might be caused by the increase of surface roughness

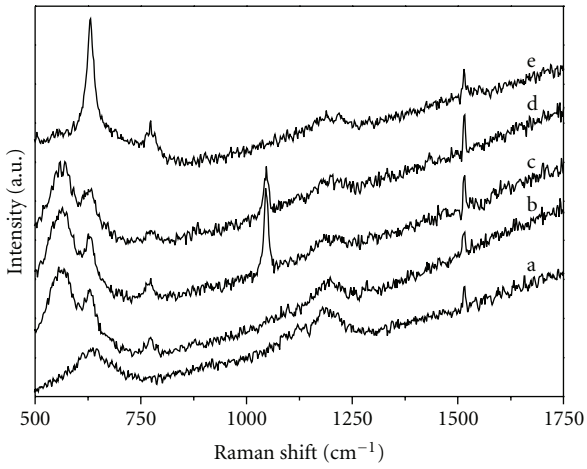

Figure 3: Raman spectra of the electrodeposited SnO_2 films obtained at different conditions, (a) untreated, (b) pure water vapour treatment, (c) HNO_3 treatment, (d) UV-treatment, and (e) calcined at 550°C.

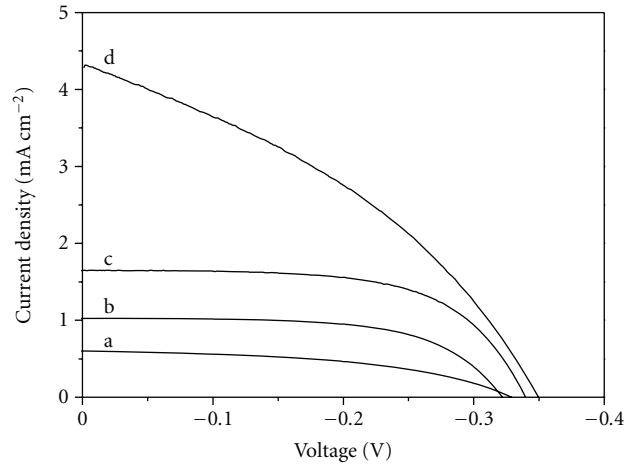

Figure 4: Photocurrent-voltage characteristic for DSCs based on the electrodeposited SnO_2 films obtained at different conditions, (a) pure water vapour treatment, (b) HNO_3 treatment, (c) UV-treatment, and (d) calcined at 550°C.

(shown in Figure 3) which permitted more single molecular absorption on the SnO_2 film. The reason was that some SnO_2 nanoparticles might be etched away during the HNO_3 treatment. The enhancement of the fill factor should be related with the better crystallization and desorption of the surface-absorbed water. After the UV-treatment, the J_{sc} was significantly increased to be 1.65 mA cm^{-2}. The conversion Efficiency was improved from 0.09% of the pure water treated SnO_2 film to 0.35% of the film after UV-treatment which was contributed to the enhancement of the crystallinity (shown in Figure 1). This conversion efficiency was expected to be further increased by the optimization of the water vapour and UV-treatment conditions, such as the water vapour pressure, the concentration of HNO_3, and UV-treatment time. It can be seen that the photoelectric properties of the SnO_2 films is possible to give a comparable performance with the films sintered at 550°C (0.56%) [25].

To further explore the effect of the post treatments on the electron transport performance, electrochemical impedance of these SnO_2 films was investigated. Impedance spectra of these DSCs are shown in Figure 5. Generally, the impedance spectrum of testing cells consisted of three main components, which were attributed to charge transfer at Pt/electrolyte (ω_1), TiO_2/electrolyte (ω_2), and diffusion impedance of I_3^- in electrolyte (ω_3) [26, 27]. The characteristic frequency of (ω_2) could reflect the recombination lifetime (τ_e) of the injected electrons [28]. The characteristic frequencies (f_{max}) are 25.7, 3.7, 3.1, and 2.1 for the water vapour treatment, water vapour treatment with HNO_3, UV-treatment and high-temperature sintering, respectively. After the water vapour treatment of SnO_2 film in pure water, the electron lifetime should be much shorter than the high-temperature sintered films (according to $\tau_e = 1/2\pi f_{max}$). But the addition of HNO_3 during the water vapour treatment process improved the electron lifetime significantly. The results might be caused by the interaction of the NO_3^- and SnO_2 nanoparticles except for the better crystallination and desorption of

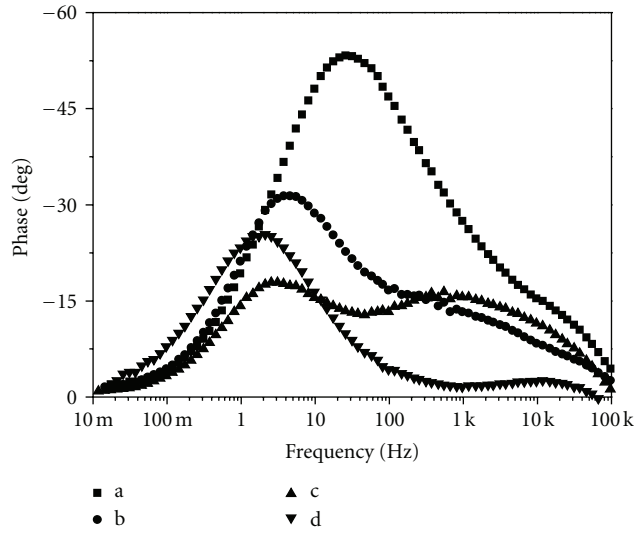

Figure 5: Impedance spectra of the electrodeposited SnO_2 films obtained at different conditions, (a) pure water vapour treatment, (b) HNO_3 treatment, (c) UV-treatment, and (d) calcined at 550°C.

the surface-absorbed water. For the surface cleaning effect of UV-treatment, the electron lifetime was further improved to be almost the same as that of the high-temperature sintered film.

4. Conclusions

SnO_2 porous films were fabricated by electrodeposition at 75°C through pulse-potential technique. These deposited films proceeded with different post treatments. The effects of the post treatments on the SnO_2 film were investigated through X-ray diffraction, FTIR-absorption spectroscopy, FE-SEM, and Raman spectra. The water vapour treatment and UV-treatment are helpful to improve the crystallinity

and to release the surface-absorbed water molecules of the electrodeposited SnO_2 film. With the addition of HNO_3 in the water vapour treatment process, the particle size was decreased and new scattering peak was found in the Raman spectra. The SnO_2 film after the combination treatment of the water vapour treatment with HNO_3 solution and UV-treatment gives a photoelectric conversion efficiency of about 0.35 with open circuit voltage 340 mV, shirt circuit current 1.65 mA cm^{-2}, and fill factor 0.63 which are all comparable with the films sintered at 550°C.

Acknowledgments

This paper was supported by the Basic and Frontier Technology Research Programs of the Department of Science and Technology of Henan Province (no. 112300410004), the Key Technologies R&D Program of Henan Province (no. 092102210005), the Nation Natural Science Foundation of China (no. 11004048), and the Research Fund of Henan University (no. 2010ZRZD07).

References

[1] B. O'Regan and M. Grätzel, "A low-cost, high-efficiency solar cell based on dye-sensitized colloidal TiO_2 films," *Nature*, vol. 353, no. 6346, pp. 737–740, 1991.

[2] A. Hagfeldt, G. Boschloo, L. Sun, L. Kloo, and H. Pettersson, "Dye-sensitized solar cells," *Chemical Reviews*, vol. 110, no. 11, pp. 6595–6663, 2010.

[3] T. Miyasaka and Y. Kijitori, "Low-temperature fabrication of dye-sensitized plastic electrodes by electrophoretic preparation of mesoporous TiO_2 layers," *Journal of the Electrochemical Society*, vol. 151, no. 11, pp. A1767–A1773, 2004.

[4] D. Wei, H. E. Unalan, D. Han et al., "A solid-state dye-sensitized solar cell based on a novel ionic liquid gel and ZnO nanoparticles on a flexible polymer substrate," *Nanotechnology*, vol. 19, no. 42, Article ID 424006, 2008.

[5] L. Liao, H. B. Lu, J. C. Li et al., "Size dependence of gas sensitivity of ZnO nanorods," *Journal of Physical Chemistry C*, vol. 111, no. 5, pp. 1900–1903, 2007.

[6] C.-L. Hsu, S.-J. Chang, Y.-R. Lin et al., "Ultraviolet photodetectors with low temperature synthesized vertical ZnO nanowires," *Chemical Physics Letters*, vol. 416, no. 1–3, pp. 75–78, 2005.

[7] Y. Y. Xi, Y. F. Hsu, A. B. Djurišić, and W. K. Chan, "Electrochemical synthesis of ZnO nanoporous films at low temperature and their application in dye-sensitized solar cells," *Journal of the Electrochemical Society*, vol. 155, no. 9, pp. D595–D598, 2008.

[8] K. Wessels, M. Wark, and T. Oekermann, "Efficiency improvement of dye-sensitized solar cells based on electrodeposited TiO_2 films by low temperature post-treatment," *Electrochimica Acta*, vol. 55, no. 22, pp. 6352–6357, 2010.

[9] B. Ferrari and R. Moreno, "Zirconia thick films deposited on nickel by aqueous electrophoretic deposition," *Journal of the Electrochemical Society*, vol. 147, no. 8, pp. 2987–2992, 2000.

[10] R. Sharma, R. S. Mane, S.-K. Min, and S.-H. Han, "Optimization of growth of In_2O_3 nano-spheres thin films by electrodeposition for dye-sensitized solar cells," *Journal of Alloys and Compounds*, vol. 479, no. 1-2, pp. 840–843, 2009.

[11] S. Karuppuchamy, K. Nonomura, T. Yoshida, T. Sugiura, and H. Minoura, "Cathodic electrodeposition of oxide semiconductor thin films and their application to dye-sensitized solar cells," *Solid State Ionics*, vol. 151, no. 1–4, pp. 19–27, 2002.

[12] H. Kim, R. C. Y. Auyeung, and A. Piqué, "Transparent conducting F-doped SnO_2 thin films grown by pulsed laser deposition," *Thin Solid Films*, vol. 516, no. 15, pp. 5052–5056, 2008.

[13] B.-Y. Wei, M.-C. Hsu, P.-G. Su, H.-M. Lin, R.-J. Wu, and H.-J. Lai, "A novel SnO_2 gas sensor doped with carbon nanotubes operating at room temperature," *Sensors and Actuators, B*, vol. 101, no. 1-2, pp. 81–89, 2004.

[14] H. J. Wang, J. M. Wang, W. B. Fang, H. Wan, L. Liu, and H. Q. Lian, "Structural and electrochemical properties of a porous nanostructrured SnO_2 film electrode for lithium-ion batteries," *Electrochemistry Communications*, vol. 11, pp. 194–197, 2010.

[15] L. Li, X. Yin, S. Liu, Y. Wang, L. Chen, and T. Wang, "Electrospun porous SnO_2 nanotubes as high capacity anode materials for lithium ion batteries," *Electrochemistry Communications*, vol. 12, no. 10, pp. 1383–1386, 2010.

[16] A. Kay and M. Grätzel, "Dye-sensitized core-shell nanocrystals: improved efficiency of mesoporous tin oxide electrodes coated with a thin layer of an insulating oxide," *Chemistry of Materials*, vol. 14, no. 7, pp. 2930–2935, 2002.

[17] S. Gubbala, V. Chakrapani, V. Kumar, and M. K. Sunkara, "Band-edge engineered hybrid structures for dye-sensitized solar cells based on SnO_2 nanowires," *Advanced Functional Materials*, vol. 18, no. 16, pp. 2411–2418, 2008.

[18] C. Prasittichai and J. T. Hupp, "Surface modification of SnO_2 photoelectrodes in dye-sensitized solar cells: significant improvements in photovoltage via Al_2O_3 atomic layer deposition," *Journal of Physical Chemistry Letters*, vol. 1, no. 10, pp. 1611–1615, 2010.

[19] P. Tiwana, P. Docampo, M. B. Johnston, H. J. Snaith, and L. M. Herz, "Electron mobility and injection dynamics in mesoporous ZnO, SnO_2, and TiO_2 films used in dye-sensitized solar cells," *ACS Nano*, vol. 5, no. 6, pp. 5158–5166, 2011.

[20] R. W. Fessenden and P. V. Kamat, "Rate constants for charge injection from excited sensitizer into SnO_2, ZnO, and TiO_2 semiconductor nanocrystallites," *Journal of Physical Chemistry*, vol. 99, no. 34, pp. 12902–12906, 1995.

[21] Y. Tachibana, K. Hara, S. Takano, K. Sayama, and H. Arakawa, "Investigations on anodic photocurrent loss processes in dye sensitized solar cells: comparison between nanocrystalline SnO_2 and TiO_2 films," *Chemical Physics Letters*, vol. 364, no. 3-4, pp. 297–302, 2002.

[22] H. J. Snaith and C. Ducati, "SnO_2-Based dye-sensitized hybrid solar cells exhibiting near unity absorbed photon-to-electron conversion efficiency," *Nano Letters*, vol. 10, no. 4, pp. 1259–1265, 2010.

[23] F. Fabregat-Santiago, J. Bisquert, G. Garcia-Belmonte, G. Boschloo, and A. Hagfeldt, "Influence of electrolyte in transport and recombination in dye-sensitized solar cells studied by impedance spectroscopy," *Solar Energy Materials and Solar Cells*, vol. 87, no. 1–4, pp. 117–131, 2005.

[24] S. Ding, Y.-L. Liu, and G. G. Siu, "Raman study of SnO_2 nanograins under different annealing temperature," *Acta Physica Sinica*, vol. 54, no. 9, pp. 4416–4421, 2005.

[25] Z. Chen, Y. F. Tian, S. J. Li, H. W. Zheng, and W. F. Zhang, "Electrodeposition of arborous structure nanocrystalline SnO_2 and application in flexible dye-sensitized solar cells," *Journal of Alloys and Compounds*, vol. 515, pp. 57–62, 2012.

[26] T. Hoshikawa, R. Kikuchi, and K. Eguchi, "Impedance analysis for dye-sensitized solar cells with a reference electrode," *Journal of Electroanalytical Chemistry*, vol. 588, no. 1, pp. 59–67, 2006.

[27] S. J. Li, Y. Lin, Z. Chen, J. B. Zhang, and X. W. Zhou, "Electrochemical impedance analysis of nanoporous TiO_2 electrode at low bias potential," *Chinese Chemical Letters*, vol. 21, no. 8, pp. 959–962, 2010.

[28] J. A. Mikroyannidis, P. Suresh, M. S. Roy, and G. D. Sharma, "New photosensitizer with phenylenebisthiophene central unit and cyanovinylene 4-nitrophenyl terminal units for dye-sensitized solar cells," *Electrochimica Acta*, vol. 56, no. 16, pp. 5616–5623, 2011.